Electronic Supplementary Material (ESI) for Dalton Transactions.

Supporting Information for

Evaluating Aqueous Flow Battery Electrolytes: A Coordinated Approach

Brian H. Robb, Scott E. Waters, and Michael P. Marshak*

*Corresponding Author: michael.marshak@colorado.edu

Table of Contents

1. Overview

The following guide is meant to demonstrate an example of how to operate a redox flow battery (RFB) for someone new to the field, and therefore provides descriptions of the basic preparation, assembly, and operation of one type of RFB (vanadium). However, this guide does not cover everything, and is not meant to be a definitive or exhaustive list of materials or equipment that can be utilized to operate an RFB or electrochemical tests that can be performed on an RFB. For example, while our flow fields are serpentine pattern (flow-by geometry), there are also various other designs that can be utilized, including interdigitated (flow-through geometry). To help provide information on other equipment or tests not included here, an "Additional Resources" section is provided at the end of the document. We are not experts on vanadium RFBs (VRFBs) and the data presented within is not intended to represent the state of the art for VRFB performance. Rather, the data presented represents the type of performance that one could expect to see for a VRFB when performing initial tests and only utilizing purchased materials. Everything within this guide can be purchased directly from suppliers and assembled and operated with the described equipment. A detailed example of such items used to operate an RFB are shown in Figure S1C. These include primary and secondary containment containers in case of leaks (Figure S1A).

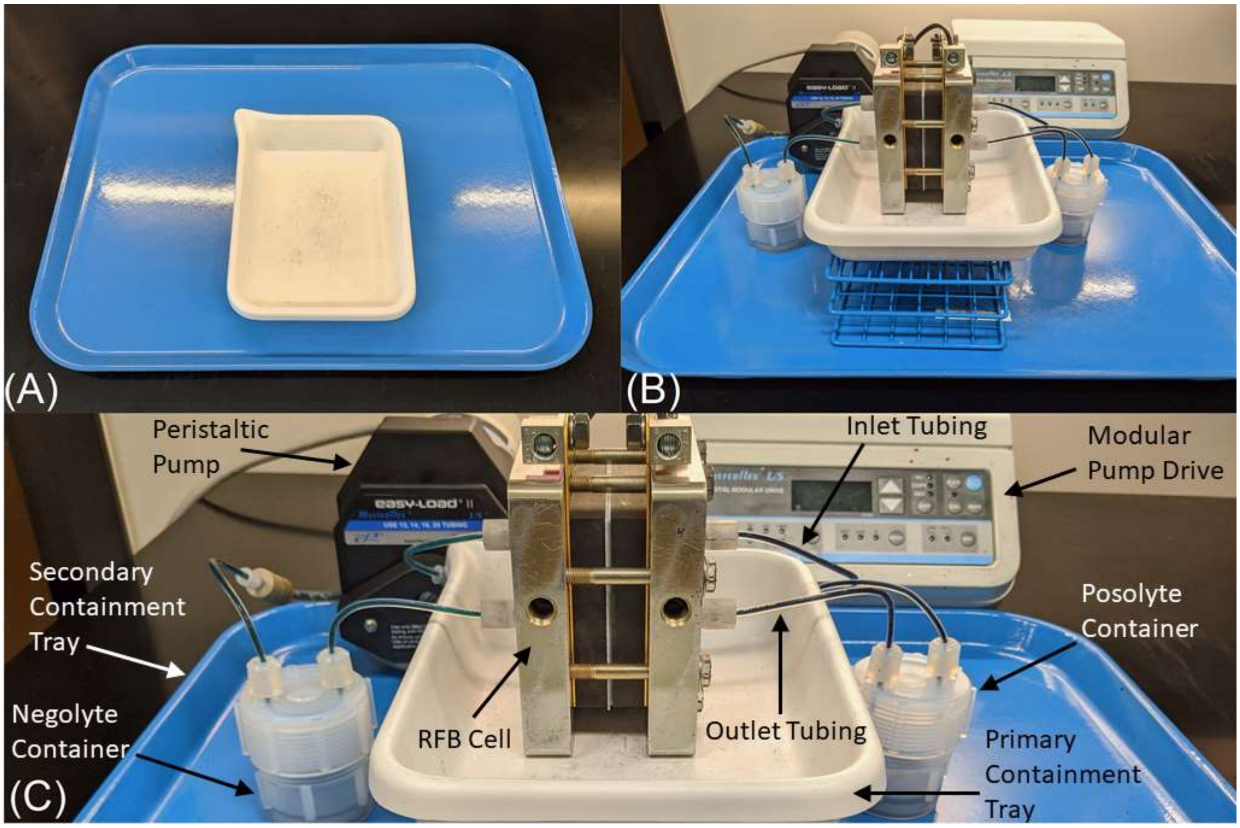

Figure S1: (A) Primary and secondary containment trays. (B) RFB setup with cell, tubing, pump, electrolyte containers, and primary and secondary containment. (C) Enlarged photograph from (B) with detailing labeling of system level components: RFB cell, peristaltic pump and modular pump drive, primary and secondary containment trays, negolyte and posolyte containers, and cell inlet and outlet tubing.

2. Parts List

The items from the following parts list are recommended for operation of an RFB, and currently cost a total of roughly $5,000. The first time a part is referenced in the main text of this document it is denoted by a **(letter)** that corresponds to the letter in this parts list. The minimum quantity of each item needed to be purchased to operate the battery are given by the **(x quantity)** in list below.

Cell – Fuel Cell Technologies (www.fuelcelltechnologies.com)
(A) (x1) 5SCH 5 cm^2 Single Serpentine Cell with Acid Configuration

Pump/Tube System – Cole Parmer (www.coleparmer.com)
(B) (x1) EW-07557-00 Masterflex L/S Precision Modular Drive with Remote I/O; 600 rpm
(C) (x1) EW-77202-60 Masterflex L/S Easy-Load® II Pump Head, SS Rotor; 2-Channel
(D) (x1) EW-06434-16 Masterflex C-Flex ULTRA Tubing, L/S 16, 25 ft. (7.6 m)
(E) (x2) EW-02023-81 Idex P-767 Peristaltic Tubing Adapter, Large Bore (2 pack)
(F) (x4) EW-12020-08 Cole-Parmer VapLock Fitting, 1/8" (3.2 mm) OD x 1/4-28 UNF(M)
(G) (x1) EW-06375-01 PFA Tubing, 1/16" (1.6 mm) ID x 1/8" (3.2 mm) OD, 25ft. (7.6 m)

Misc Parts – McMaster-Carr (www.mcmaster.com)
(H) (x1) 8569K34 Film Made From Teflon® PTFE 12" Wide x 3', 0.002" (0.051 mm) Thick
(I) (x1) 8569K48 Film Made From Teflon® PTFE 12" Wide x 1', 0.04" (1.02 mm) Thick
(J) (x1) 3488A9 Multiple-Size Hole Punch for 5/64" (2.0 mm) to 3/16" (4.8 mm) Diameter
(K) (x1) 35435A11 Precision Knife
(L) (x4) 5533K433 Compression Tube Fitting PVDF Adapter, 1/8" (3.2 mm) OD x 1/8 MNPT
(M) (x1) 4922T81 Polyethylene Plastic Pan
(N) (x1) 9764T7 Food Industry Fiberglass Pan

Membrane/Electrodes – Fuel Cell Store (www.fuelcellstore.com)
(O) (x1) 1592017 SGL Sigracet 39AA carbon paper electrode 15 x 30 cm
(P) (x1) 593263 Nafion™ 212, 30 x 30 cm

Electrolyte Containers – Savillex (www.savillex.com/en)
(Q) (x2) 500-060-02 60 mL Column Component Vessel, 1-1/2" MNPT
(R) (x2) 600-058-24 58 mm Closure, (2) 1/8" (3.2 mm) OD Tube Ports, 1-1/2" FNPT
(S) (x1) 730-0055 58 mm Wrench Set

2.1 List of Abbreviations

PTFE - Polytetrafluoroethylene
OD – Outer Diameter
ID – Inner Diameter
UNF – Unified National Fine
PFA - Perfluoroalkoxy alkanes
PVDF - Polyvinylidene difluoride
MNPT/FNPT – Male National Pipe Threads/Female National Pipe Threads

3. Vanadium Electrolyte Preparation

The following procedure was used to prepare the electrolyte solutions that are used in this guide. This is not the traditional industry method of making a VRFB electrolyte, which instead uses a commercially available premixed electrolyte of $V^{3.5+}$ and utilizes a precharging/rebalancing step.

3.1 Positive Electrolyte (V^{4+}/V^{5+})

1.5 M V^{4+} as $[VO(H_2O)_5]^{2+}$: A stirred solution of 5 M H_2SO_4 (10 mL) is sparged with N_2 for no less than 10 mins before V_2O_5 (0.682 g, 3.75 mmol, 0.25 eq) and V_2O_3 (0.562 g, 3.75 mmol, 0.25 eq) are slowly added under a positive flow of N_2. The vessel is sealed, and the solution is stirred at 80 °C for 2 h to dissolve. The concentration of the blue solution is confirmed via absorption spectroscopy ($\varepsilon = 13.4$, 765 nm). Note that high V(V) concentration can cause carbon oxidation.

3.2 Negative Electrolyte (V^{2+}/V^{3+})

1.5 M V^{3+} as $[V(H_2O)_6]^{3+}$: A stirred solution of 5 M H_2SO_4 (10 mL) is sparged with N_2 for no less than 10 mins before the slow addition of V_2O_3 (1.124 g, 7.5 mmol, 0.5 eq) under a positive flow of N_2. The vessel is sealed, and the solution is stirred at 80 °C for 16 h to dissolve. The concentration of the green solution is confirmed via absorption spectroscopy ($\varepsilon = 5.85$, 610 nm).

4. Flow Cell Preparation

4.1 Overall Cell Parts and Operation:

A 5 cm^2 single-cell flow battery **(A)** was utilized with the acid cell configuration, so that the tubing carrying the electrolyte feeds directly into the graphite flow plate without contacting the aluminum or stainless-steel cell components. The cell comes from the supplier with aluminum end plates, gold-plated copper current collectors with an insulating layer on one side (electrically insulated from the aluminum end plates) (Figure S2B), and graphite flow plates with a serpentine flow field (Figures S2C, S2D). The original connectors to the aluminum end plates from the suppliers is a stainless steel Swagelok fitting, but this was replaced with a PVDF fitting **(L)** to allow for easier tubing replacement (Figure S2A).

The cell also comes with an AC voltage heating unit that is composed of two heaters that can be inserted into each aluminum end plate to heat the cell (Figure S3). Heaters were not utilized for any of the experiments within this guide and require the purchase of additional equipment to permit temperature control.

The flow plates comprised Poco graphite blocks with 5 cm^2 single serpentine flow fields. All electrolytes were pumped into and out of the flow cell using a two-channel peristaltic pump **(C)** and peristaltic pump digital modular drive **(B)**. Flow cell experiments were conducted using a Gamry Interface 5000E potentiostat/galvanostat but can be operated with many standard potentiostat/galvanostat units.

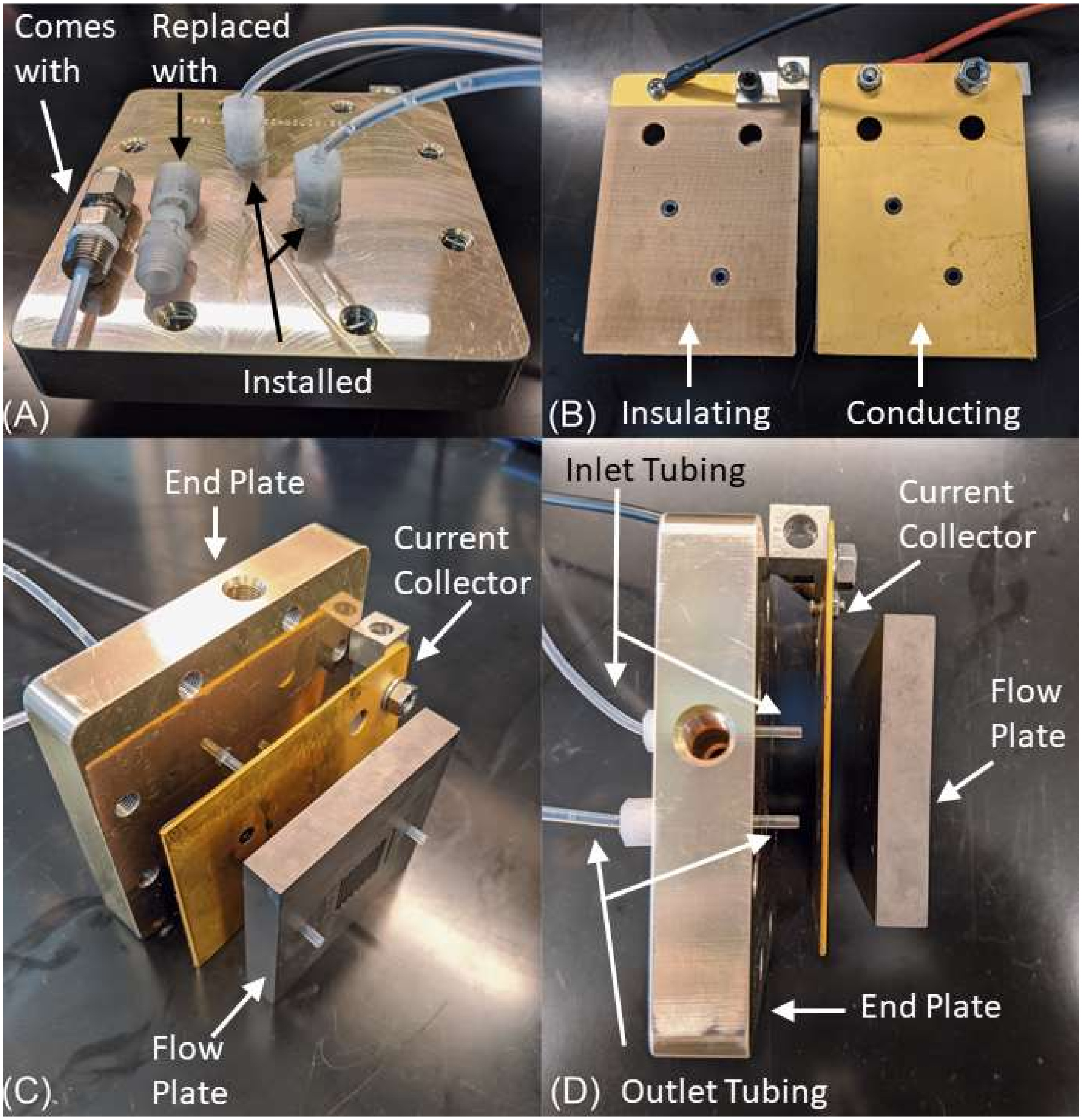

Figure S2: (A) Aluminum end plate with original metal Swagelok fitting (left), disassembled PVDF fitting (middle), and two installed PVDF fittings (right). (B) Front and back of gold-plated copper current collector, showing the insulating (left) and conductive (right) sides. (C) Half of the flow cell setup, showing (from left to right) the aluminum end plate, gold-plated copper current collector (insulating side facing the aluminum plate and conductive side facing the graphite flow plate), and the graphite flow plate. Cell is shown on its side. (D) Vertical view of the parts from part (C). Note the length of PFA tubing that goes through the end plate to be able to feed into the graphite flow plate.

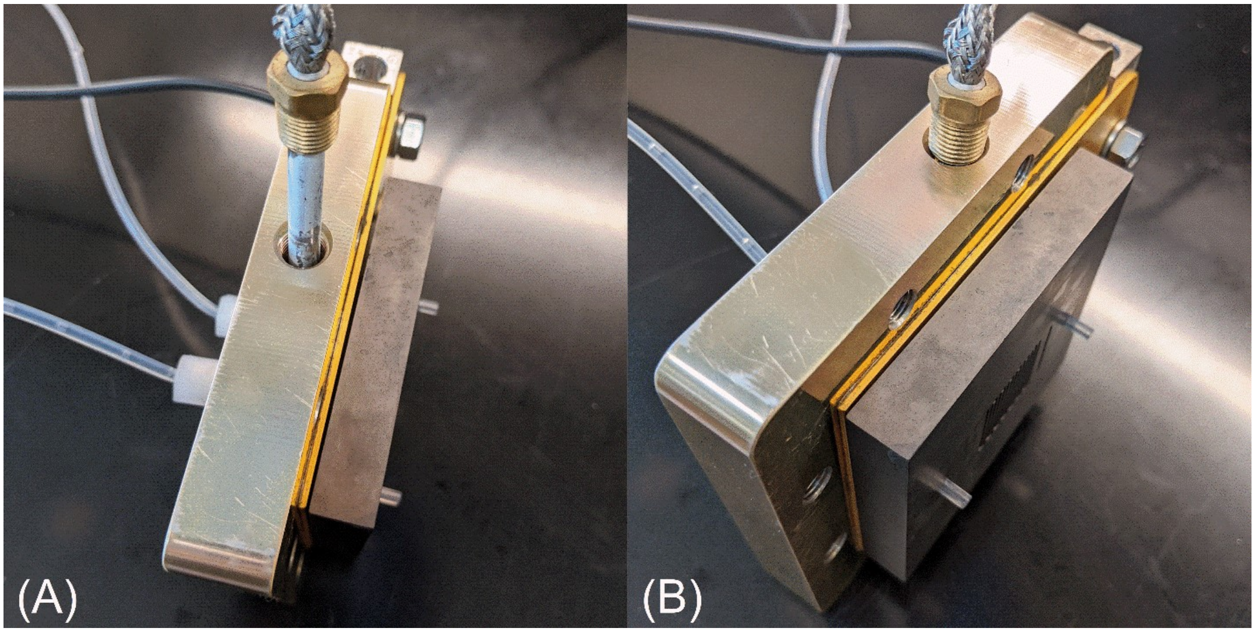

Figure S3: (A) Cell heater being inserted into the aluminum end plate. (B) Cell heater after insertion but before being tightened.

4.2 Initial Flow Cell Part Preparation:

Prior to operating the cell for the first time, there are initial preparation steps that must be performed that are not required on subsequent operations. These include preparing membrane and electrode gaskets as well as preparing and installing the tubing that will carry the electrolyte solutions. Our standard setup, which utilizes 0.04” thickness PTFE gaskets for each set of 5 carbon paper electrodes, and a single 0.002” PTFE gasket for a single Nafion 212 membrane will be used as an example, but the same preparation method will work for any gasket size. Large sheets of PTFE film can be purchased in various thicknesses from McMaster-Carr and cut down to smaller individual gasket size. Proper gasket thickness is required to ensure appropriate compression of the carbon paper and minimization of the cell electrical resistance.[1] When utilizing five stacked sheets of the carbon paper discussed in this guide, the 0.04” gaskets will provide 27% compression.

4.3 Gasket Preparation

A stencil that mirrors the tubing hole location and flow field location of the flow plates is provided with the flow battery. A precision knife **(K)** is used to cut the PTFE gaskets. First, two 0.04” PTFE squares are cut from the large sheet of 0.04” PTFE film **(I)** using the outer shape of the stencil, which makes the square the same size as the flow plate (Figure S4). The stencil is then used to cut an inner square, approximately 2.24 cm × 2.24 cm and represents the location of the flow field and is the place where the carbon paper electrodes will be placed during cell assembly. A revolving leather hole punch tool **(J)** is then used with the stencil to punch holes into the gasket that align with the guide tubing that lines up the two flow plates. The same process is then repeated with a single sheet of 0.002” PTFE film **(H)** to create the membrane gasket, except the 2.24 cm × 2.24 cm inner square is widened to 4 cm × 4 cm to allow for the larger membrane to fit.

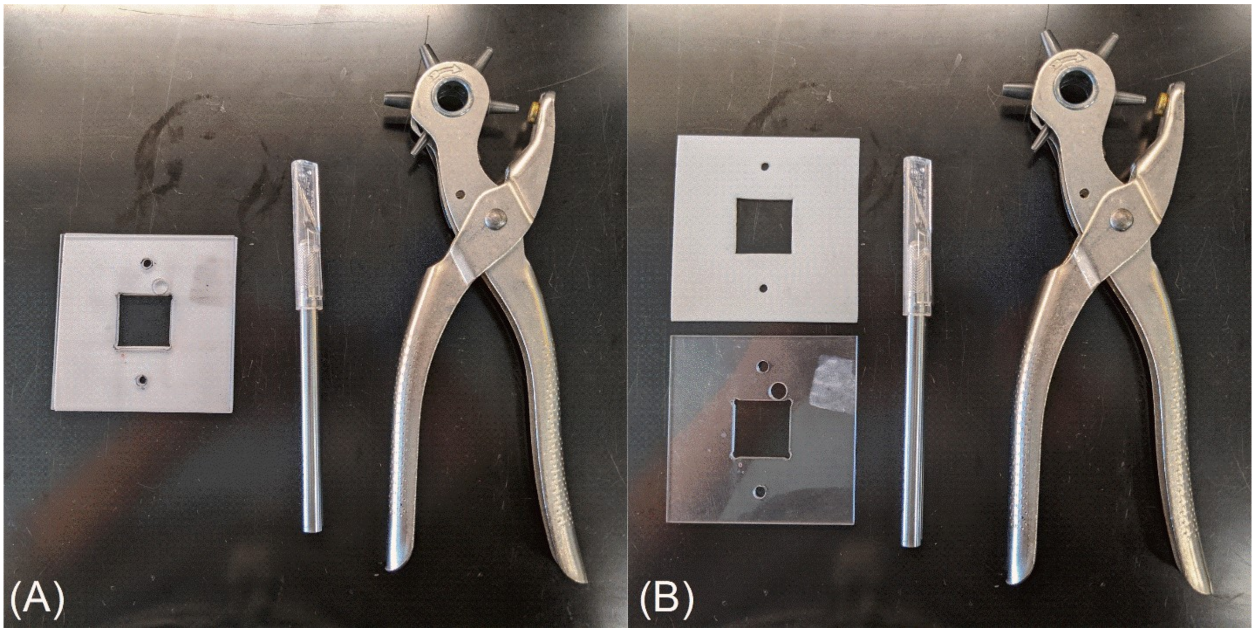

Figure S4: (A) The provided stencil on top of a cut gasket, with a precision knife and leather hole punch. (B) The finished cut gasket (white) with the stencil (clear), and the precision knife and leather hole punch.

4.4 Tubing Connections

To insert the PFA tubing **(G)** into the cell for the first time, the PVDF adapters are first installed into the outer plates of the flow battery (Figure S2A). The compression fitting section is removed from the adapter and placed onto PFA tubing, and that PFA tubing is then fed through the PVDF adapter and outer plate of the flow battery to where it would go into the graphite flow plate (should extend approximately ¼" or 6.4 mm) (Figure S2D). The current collector and graphite flow plate can be used as a guide to how far the tubing should be fed. The graphite flow plate should be able to lay flush against the current collector when the tubing is inserted into the back of the flow plate. Once the tubing is fed to the right depth, the compression fitting is then tightened onto the PVDF adapter to hold the PFA tubing in place. Four pieces of PFA tubing will need to be run this way, as the inlet and outlet for each side of the battery. The top PFA tubing is the inlet to the flow plate and will attach to the tubing at the outlet of the peristaltic pump (Figure S1C). The bottom PFA tubing is the outlet from the flow plate and will go to the electrolyte reservoir (Figure S1C). Cut each piece of PFA tubing to the desired length, depending on the distance of the pump and electrolyte reservoirs to your flow cell. For tests utilizing small volumes, it is recommended to minimize the length of tubing used and therefore the required dead volume of electrolyte solutions. It is crucial that the fittings are tight and secure to prevent electrolyte leakage and air (O_2) permeation. Liquid leaks will change the solution volume over time and affect the total electrolyte capacity. Liquid leak checking can be performed by running colored fluid through the tubing and checking for leaks. Air leaks into the system will impact O_2 sensitive materials such as V^{2+} or V^{3+} and can affect efficiencies as well as electrolyte capacity over time. It may be necessary to run sensitive tests within an air-free glovebox to minimize O_2 permeation.[2]

To connect the PFA tubing to the peristaltic pump tubing use the following process (Figure S5). First cut two lengths of the Masterflex C-Flex Ultra **(D)** peristaltic tubing to a length that will allow you to use it with your pump setup. At both ends of each peristaltic tubing, attach the peristaltic tubing adapters **(E)** (Figure S5B) by unscrewing the outer threaded piece and placing the outer threated piece and insert onto the peristaltic tubing (Figure S5C). Then, fit the peristaltic tubing onto the conic hose barb section of the adapter piece (Figure S5C) and retighten the threaded pieces to create a seal (Figure S5D). Next, put a tubing adapter **(F)** onto the end of each PFA inlet tubing from above (Figure S5A), and then connect each inlet tube to a separate piece of peristaltic tubing by threading the adapter into the peristaltic tubing adapter (Figure S5E). Two new pieces of PFA tubing should now be cut, which will go from the electrolyte reservoirs to the inlet of the pump. Connect these PFA tubing pieces to the other ends of the two pieces of peristaltic tubing using the same **(F)** adapters and procedure as above.

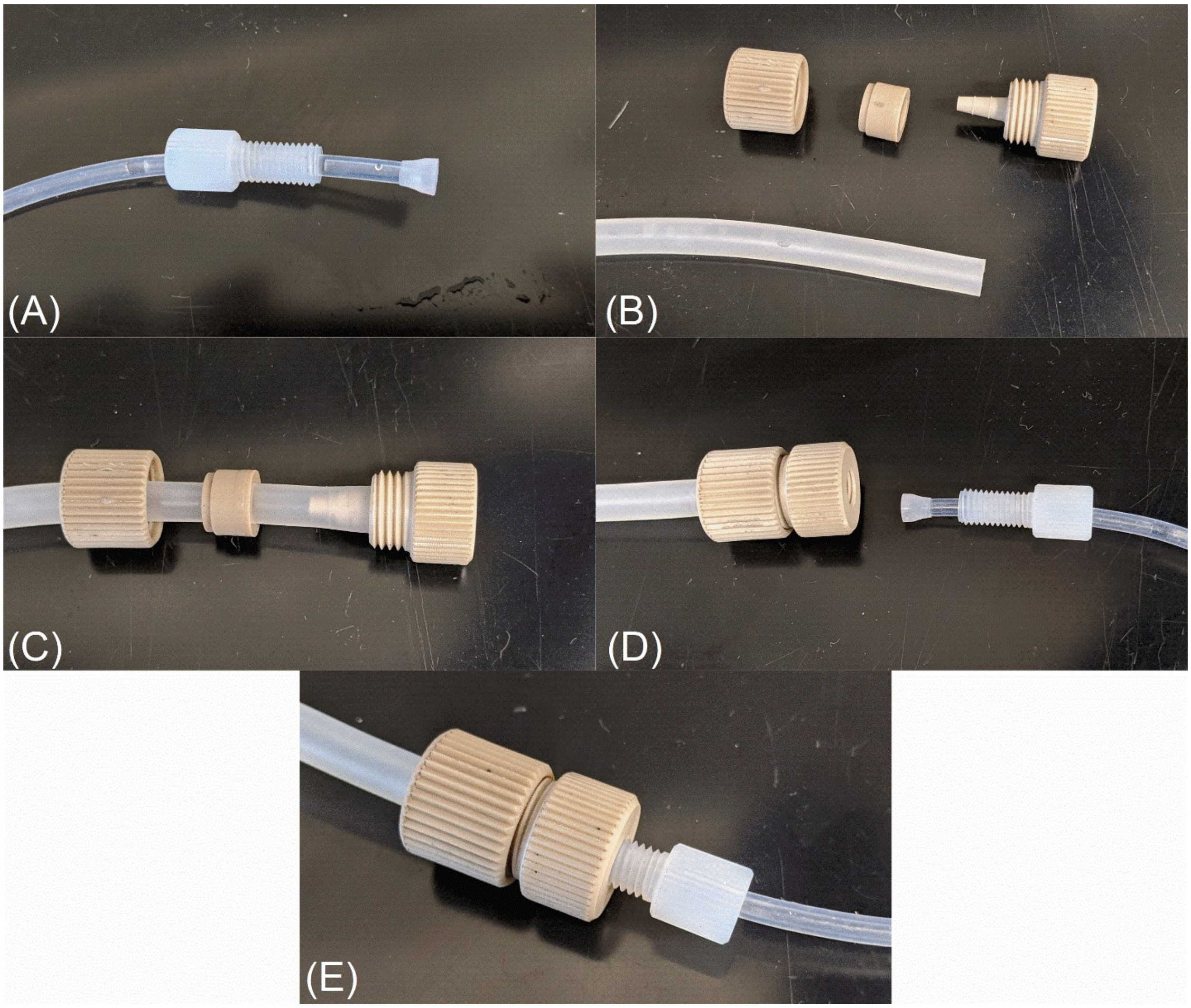

Figure S5: (A) UNF fitting for 1/8” OD PFA tubing. (B) L/S 16 tubing with disassembled compression fitting. (C) L/S 16 tubing with compression fitting fit onto tubing. (D) Assembled compression fitting on L/S 16 tubing and fitting on 1/8” OD PFA tubing. (E) Fully assembled fitting to join L/S 16 tubing to 1/8” OD PFA tubing.

4.5 Operation Flow Cell Part Preparation:

Prior to operation of the flow cell, an electrode material and membrane material must be purchased. This preparation method will describe our typical setup used, with carbon paper **(O)** as the electrode material and a Nafion cation exchange membrane **(P)** as the membrane material. Both can be purchased as large sheets from Fuel Cell Store. Once these materials are acquired, the following procedure can be used to prepare them for use.

The stencil guide and precision knife are used to cut the large carbon paper sheet into approximate 2.24 cm × 2.24 cm squares, which will fit into the inner square of the gasket material (Figure S6A). The carbon paper squares are kept in an oven at 150 °C to improve wettability. A ruler and scissors are then used to cut approximately 3.3 cm × 3.3 cm squares of the membrane from the large sheet. The membrane and associated plastic backing films (front and back) are completely submerged in DI H_2O for at least 12 h, until the membrane has swelled and separated from the plastic casings (Figure S6B). Once these steps have been completed, the cell is ready to be assembled.

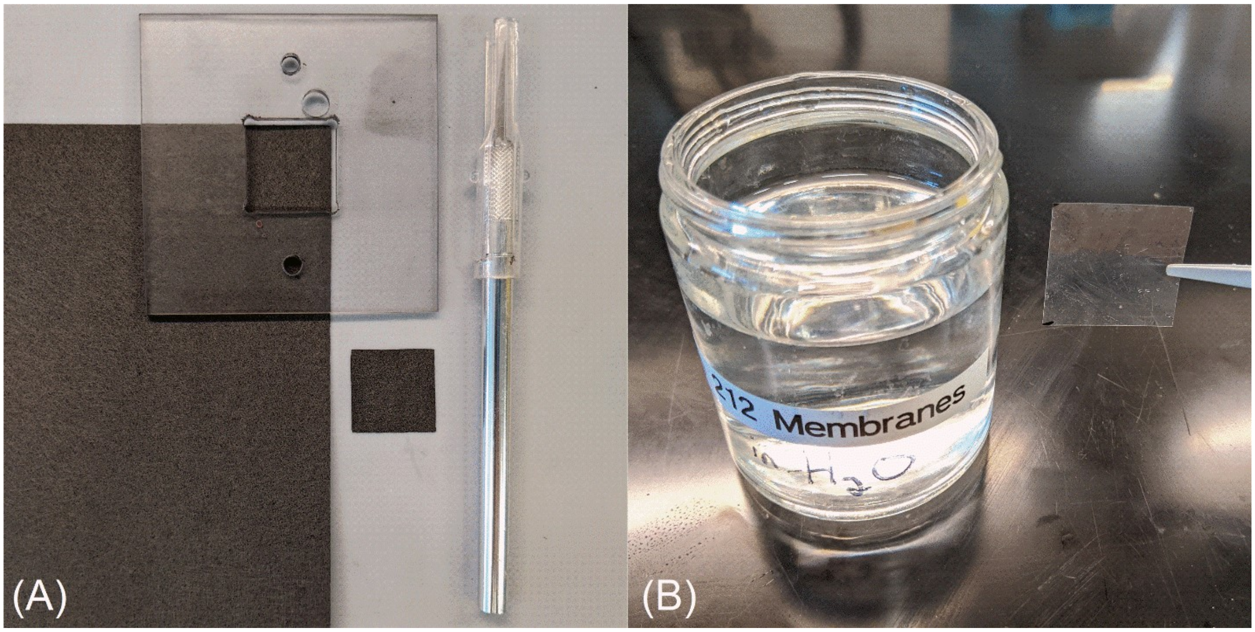

Figure S6: (A) Stencil and precision knife illustrating how 5 cm^2 carbon paper squares are cut for use in the RFB. (B) 3.3 cm × 3.3 cm membrane with two plastic backing pieces held by plastic tweezers and shown before placing in a water bath to soak overnight.

4.6 Cell Assembly

To assemble the flow cell, first place both graphite flow plates onto their associated end plate, making sure that the current collector is correctly installed with the insulating side touching the end plate (each flow plate will only fit onto one of the end plates) (Figure S7).

One of the flow plates will have the PFA guiding tubing attached (Figure S7B). Starting with this flow plate, place one of the electrode gaskets (0.04”) onto the guiding tubing (Figure S8A). Next, 5 carbon paper sheets are rinsed with DI H_2O and then stacked and placed inside of that gasket inner square cutout (note, remove the carbon papers from the oven and allow them to cool before handling) (Figure S8B). When operating the RFB, electrolyte flows from the top of the flow field, through the channel, then out through the bottom hole in the flow field. It is essential that inlet and outlet tubes are appropriately placed. The membrane gasket (0.002”) is then placed onto the guiding tubing and a membrane is then removed from the DI H_2O with plastic tweezers and placed on top of the carbon papers while not overlapping the membrane gasket (Figure S8C).

The plastic casings that are removed from the membrane DI H_2O are discarded. The other electrode gasket is then placed onto the guiding tubing (Figure S8D), and 5 more pieces of carbon paper are rinsed with DI H_2O and then stacked and placed inside the inner cutout of the gasket (Figure S8E). Finally, the flow plate, current collector, and end plate assembly is then placed onto the guiding tubing and pressed together so that everything should be flush (Figure S8F). Do so gently to avoid crushing the guiding tubing. The 8 bolts are then inserted into the end plates in a star pattern and fastened finger tight followed by tightening with a torque wrench to 13.6 N m (10 ft lb). Detailed bolt tightening methods for cell assembly are explained below in Figure S9. Once bolted together, the RFB cell is now assembled and ready to be used (Figure S10).

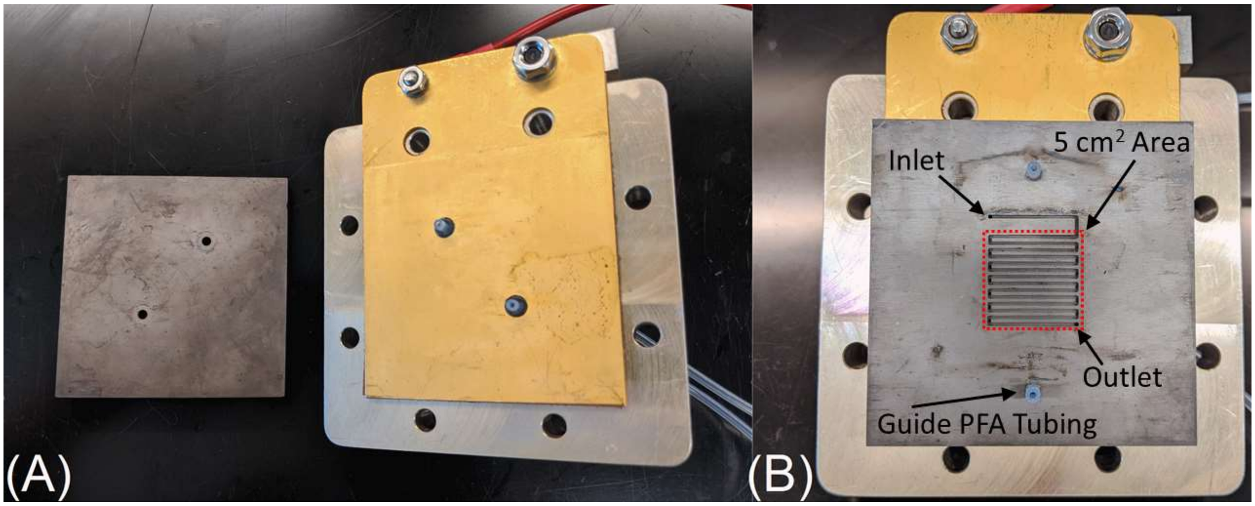

Figure S7: (A) Back of graphite flow plate showing the holes that align with the PFA tubing coming through the end plate and current collector. (B) Front of the graphite flow plate showing the inlet (top) and outlet (bottom) of the flow plate as well as the 5 cm^2 active area and guide PFA tubing. The inlet area is covered by the gasket and it is important to not pump the system backwards because fluid flowing in through the uncovered outlet could damage the electrodes or membrane.

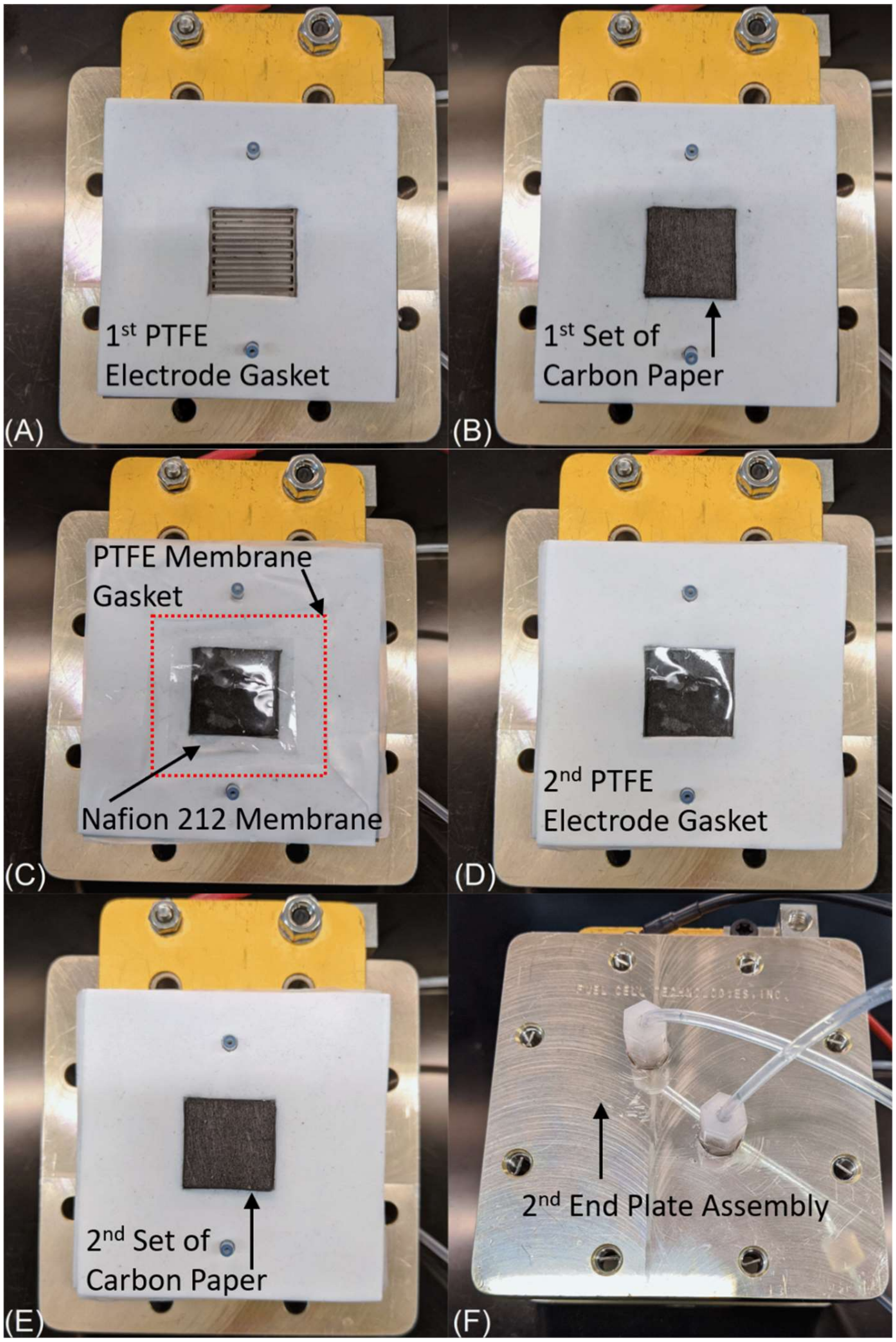

Figure S8: (A) 1st PTFE electrode gasket placed on top of 1st flow plate. (B) 5 carbon paper electrodes placed inside the 1st electrode gasket. (C) PTFE membrane gasket and Nafion 212 membrane placed on top of electrodes and 1st electrode gasket. The dashed red line illustrates the inner position of the PTFE membrane gasket as to not overlap the membrane. (D) 2nd PTFE electrode gasket is placed on top of the membrane gasket and membrane. (E) 2nd set of 5 carbon paper electrodes placed inside 2nd electrode gasket. (F) 2nd end plate assembly (2nd flow plate, 2nd current collector, and 2nd end plate) is placed on top of electrodes and 2nd electrode gasket.

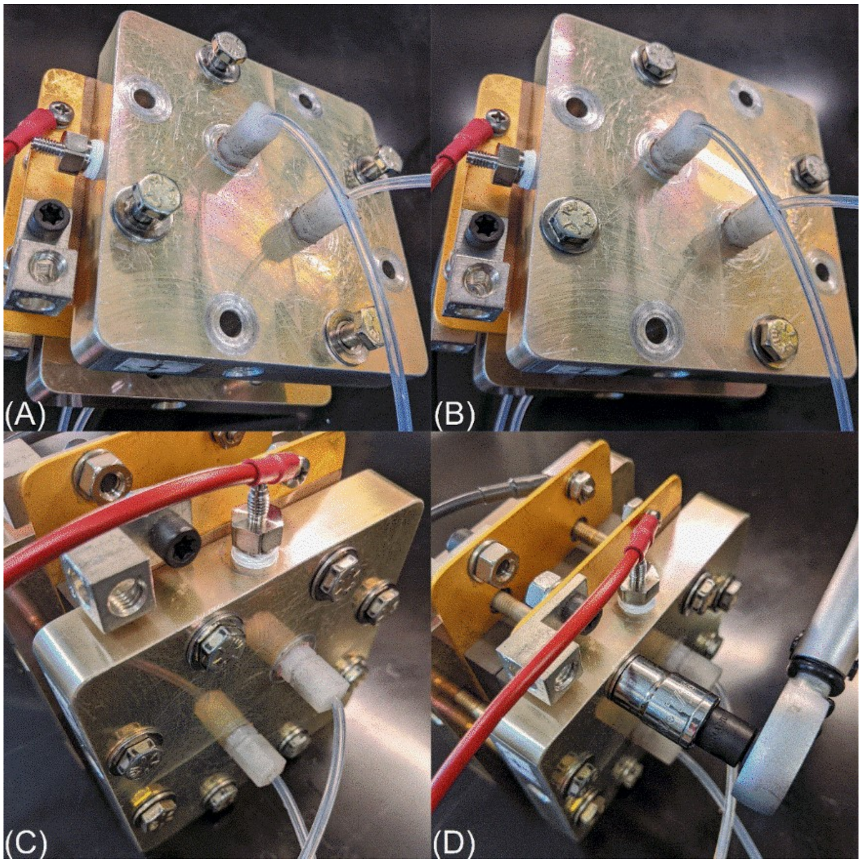

Figure S9: (A) 4 of the bolts inserted in an alternating pattern. (B) 4 of the bolts fastened finger tight. (C) The remaining 4 bolts are inserted and fastened finger tight. D) A torque wrench used to tighten the bolts in a star pattern to the desired torque.

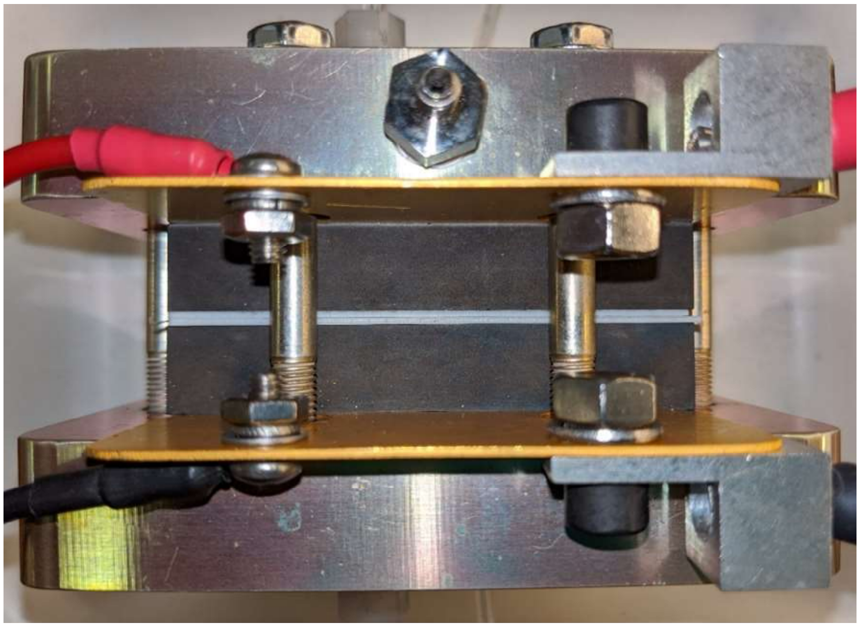

Figure S10: Fully assembled RFB cell showing proper configuration.

4.7 Electrolyte and Cell Nitrogen Flush

During operation, electrolyte solutions are contained in 60 mL PFA bottles/containers **(Q)** with 58 mm caps/lids **(R)**. Prior to transferring the electrolyte solutions to the PFA containers, the containers are pre-purged with N_2 by the following procedure: lightly tightening the lid onto a container, fully inserting a PFA tube into the container through a 58 mm cap compression fitting, connecting the PFA tube to a nitrogen source, and turning on the N_2 flow to flush the bottle with N_2. With the N_2 flowing, the lid is then quickly loosened and slightly lifted (the PFA tubing should remain in the container), the electrolyte solution is quickly added, and the lid is then closed and retightened. The N_2 tube is lowered into the solution to maintain bubbling. The lid is then fully tightened onto the PFA bottles using the 58 mm Wrench Set **(S)** (Figure S11A).

The RFB cell inlet PFA tube is then threaded through the second, open 58 mm cap compression fitting into the container headspace (do not insert into electrolyte solution during purge as the N_2 headspace pressure will force fluid to flow through the cell and cause electrolyte loss) and the compression fitting is tightened (Figure S11B). This will flow N_2 through the tubing and cell to purge the system of any air.

After 5 minutes, the N_2 purge tubing is quickly removed (leaving the compression fitting on the cap) and the RFB cell outlet PFA tubing is quickly inserted. The inlet PFA tubing is then adjusted to be in the electrolyte solution, and the compression fittings on both the inlet and outlet tubing are tightened to the cap. The N_2 flow can now be turned off.

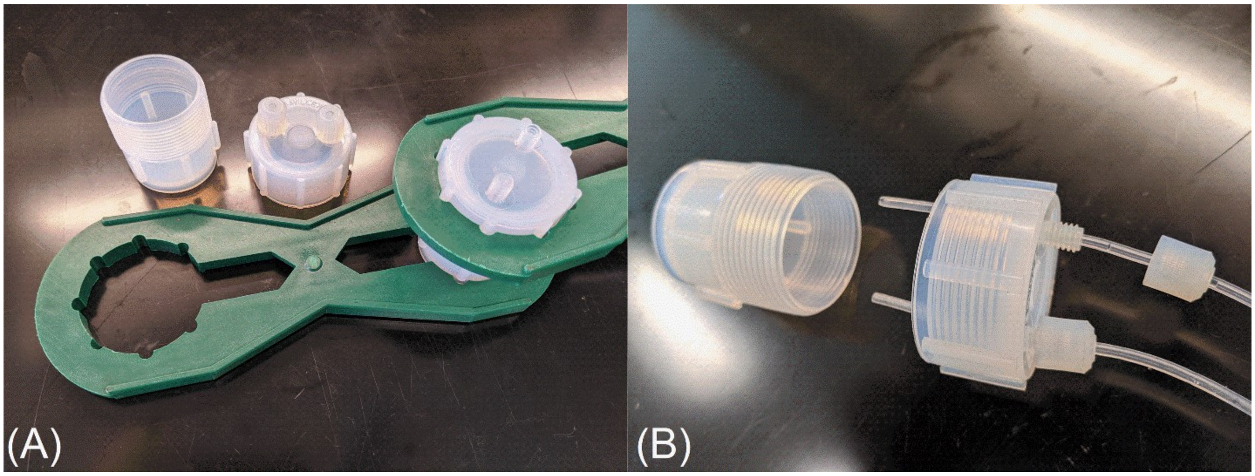

Figure S11: (A) PFA caps are tightened to the PFA containers using the provided wrenches. (B) PFA tubing is threaded through the cap and tightened with the compression fittings on the right. This is representative to show the tubing inserted through the cap, as the cap will be sealed to the container at this point. Note, one tubing hole on the PFA cap may need to be drilled out to allow for tubing to pass entirely through.

4.8 Final Cell Preparation

Once the RFB cell and electrolyte containers are fully assembled and connected, the RFB cell is placed into the primary containment tray **(M)**. The primary containment tray and the two electrolyte containers are then placed in the secondary containment tray **(N)** (Figure S1B). The L/S 16 tubing is then loaded into the peristaltic pump head and the peristaltic pump head is closed. The peristaltic pump motor is connected to the digital modular drive with a cable. The digital modular drive is set to the required rotations per minute (RPM) setting to achieve the desired liquid flow rate, and then turned on. This causes the electrolyte solutions to pump through the tubing and cell. The RFB cell is now ready for electrochemical testing by following the electrochemical procedures section below.

4.9 Cell Cleaning

Following cell cycling, the vanadium solutions are drained back into the PFA bottles by slightly unscrewing the compression fitting on the inlet tube and lifting the tube above the solution level. If the solutions are to be used in further tests or need to remain air-free, the electrolyte reservoir (PFA bottle) can remain air-free by not fully removing the inlet tubing from the PFA bottle during the previous draining step, and then retightening its compression fitting. To clean the cell, the PFA tubes are then removed from the reservoirs by unscrewing the compression fittings on the reservoirs and approximately 20 mL of 5 M HCl is flushed through each side of the cell to remove any residual vanadium solution without causing vanadium solids to precipitate. Following the acid rinse, 50 mL of DI H_2O is flushed through each side of the cell to remove any residual acid.

If there is any reason to believe that vanadium solids were precipitated out during flow battery operation, the cell can be allowed to sit with 5 M HCl within for approximately 12 h to dissolve the solids. It is important to note that this type of graphite flow plate can be damaged by extended exposure to concentrated nitric or sulfuric acid, therefore, HCl is recommended for cleaning these types of plates. If utilizing other flow plate materials, a chemical/material compatibility guide or the flow plate manufacturer should be consulted prior to cleaning to determine what cleaning solutions can be utilized. The above rinsing procedure is then repeated, with 20 mL of 5 M HCl followed by 50 mL of DI H_2O, followed by the cell being disassembled.

If there is no evidence that the carbon papers or membrane have been compromised (cell performance and resistances remained the same throughout testing), the cell may reused in this state without disassembling so long as the membrane does not dry out and is kept hydrated by pumping water into the cell and allowing it to sit in the RFB and tubing. If there is evidence that the carbon paper or membrane is compromised, contaminated, or otherwise no longer useable, then the cell must be disassembled. Upon disassembly, the gaskets and carbon plates are wiped with Kimwipes. They are then rinsed with DI water and dried with compressed air. This process is repeated with isopropanol. If any loose particulate remains, it may be removed with plastic tweezers or small amounts of compressed air. It is important to use soft materials for cleaning that will not scratch the graphite plates. The cell is now ready for reassembly using the method above.

5. Electrochemical Procedures

Various electrochemical experiments for quantifying RFB performance will now be described. These electrochemical experiments include linear sweep voltammetry (LSV), cell cycling via chronopotentiometry, and open circuit voltage (OCV) measurements. These experiments show RFB data such as charging or discharging voltage, maximum power output, and cycling efficiencies such as coulombic efficiency, voltage efficiency, and energy efficiency. LSV will sweep from a start to end voltage at a set rate, analogous to cyclic voltammetry, but in only one direction. LSV demonstrates the current-voltage behavior of the cell. A linear response corresponds to ohmic behavior and be fit to give a cell polarization resistance which can allow the calculation of power density vs current density. OCV will record cell voltage as a response to changing state of charge (SOC). A Nernstian response, sigmoidal, is expected for a changing concentration. The cell is at its equilibrium voltage at 50% SOC, which should be reported when discussing new chemistries (not reported here as VRFB equilibrium voltage is known and widely reported). Galvanostatic charging and discharging, or chronopotentiometry, allows one to monitor cell voltage as a function of time with an applied current through charge and discharge cycles. This experiment can demonstrate current, voltage, and energy efficiencies. For many RFB tests, often one electrolyte is in excess in order to study the performance of the other electrolyte.

5.1 Initial Assembly

Once the flow battery itself has been assembled as described in the previous section, the RFB needs to be connected to the potentiostat electrical leads. The Gamry potentiostat that was utilized for the presented data has 5 leads that are connected to the RFB: working (green/teal), working sense (blue), counter (red), counter sense (orange), and reference (white) (Figure S12). The configuration used for these tests had the counter, counter sense, and reference leads attached to the negolyte side (V^{2+}/V^{3+} side) and the working and working sense leads connected to the posolyte (V^{4+}/V^{5+} side). This arrangement results in a positive voltage when operating the RFB and as well as a positive charging current and a negative discharge current.

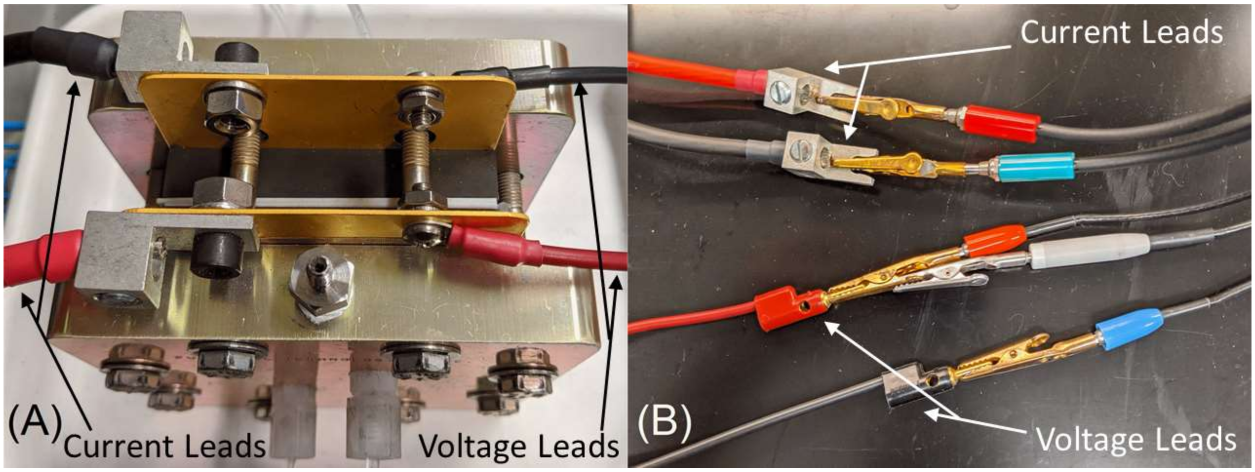

Figure S12: (A) Assembled RFB illustrating the current and voltage leads attached to the cell. (B) Potentiostat leads connected to red (negolyte) and black (posolyte) current and voltage leads of the RFB. It is important that the sets of leads do not make contact throughout testing.

5.2 Linear Sweep Voltammetry and Power Performance

Typically, one of the first experiments performed for an RFB starting in a discharged state is LSV. This test involves applying a voltage and measuring the resulting current produced in the battery. When performing a linear sweep, the potentiostat applies an initial voltage and then sweeps the voltage at a specific rate to a defined ending voltage, analogous to half of a cyclic voltammetry experiment. An example of this test with a fully discharged VRFB battery is shown below (Figure S13). This test will determine what charging currents are able to be applied and at what the initial voltage would be at those currents. For instance, in the attached plot, if the RFB started charging at 0.4 A cm^{-2} the initial charging voltage would be expected to be approximately 1.63 V. Additionally, LSV can reveal possible cell issues which may be seen as unexpected peaks from impurities or lower than expected current from additional cell resistances such as an improperly installed membrane or electrodes. One needs to be aware that performing LSV will charge the battery, which may be significant at small volumes and/or low concentrations. If the subsequent test after an LSV requires a fully discharged battery at 0% state of charge (SOC), one will want to apply a constant voltage discharge before further testing to ensure that the cell is fully discharged. If the electron transfer kinetics of charging and discharging vary greatly, linear sweep voltammetry can also be used at high states of charge to determine what discharge currents can be applied.

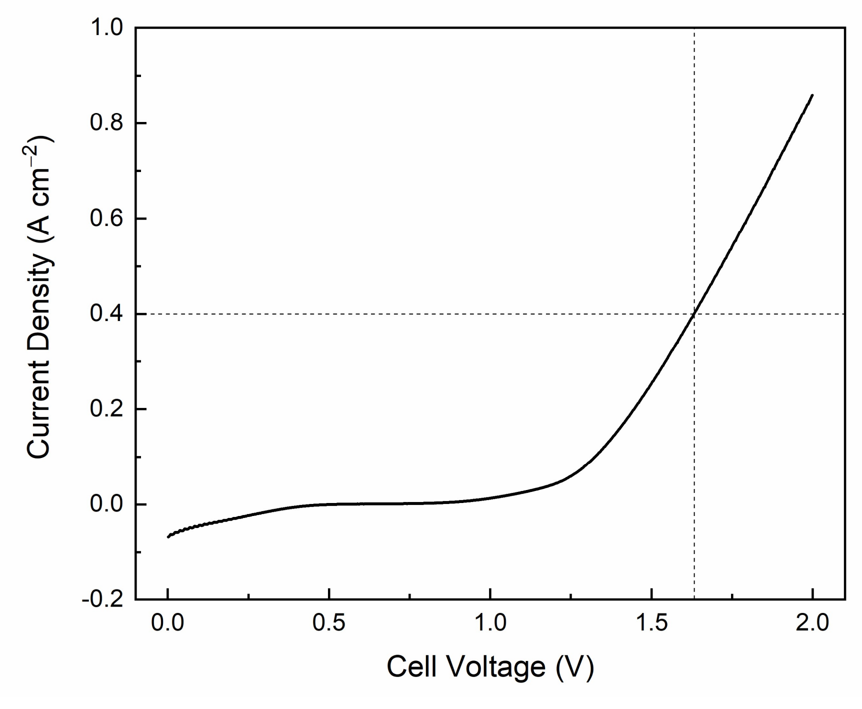

Figure S13: Low SOC LSV for a 1.5 M V^{3+} and 1.5 M V^{4+} RFB.

An additional use for LSV is to assess the power performance of an RFB. This is done by performing LSV at varying SOC. It is expected that at the maximum state of charge, a maximum discharge power output can be achieved. To perform this experiment, the RFB is charged to a specific SOC and LSV is performed from the OCV to a low voltage. Similar to an initial LSV, the voltage cutoffs used will depend on the active-species used and the solvent window. When looking at power output only, the LSV test is started at the open circuit voltage and the voltage is swept toward 0 V. Due to the slight change of SOC from the LSV, the battery should then be discharged fully. This process is repeated to record power data at the desired SOCs. The LSV will provide a plot of Cell Voltage (V) vs. Current (A) that can be converted to Current Density (A cm^{-2}) vs. Power Density (W cm^{-2}). Examples of a high SOC LSV plot and power curve plot for the VRFB described utilizing a 5 cm^2 cell are shown below (Figure S14A, B). Depending on the stability of the material that is being used, it can be advantageous to collect an OCV before performing a LSV at each SOC to ensure that the desired SOC has been reached.

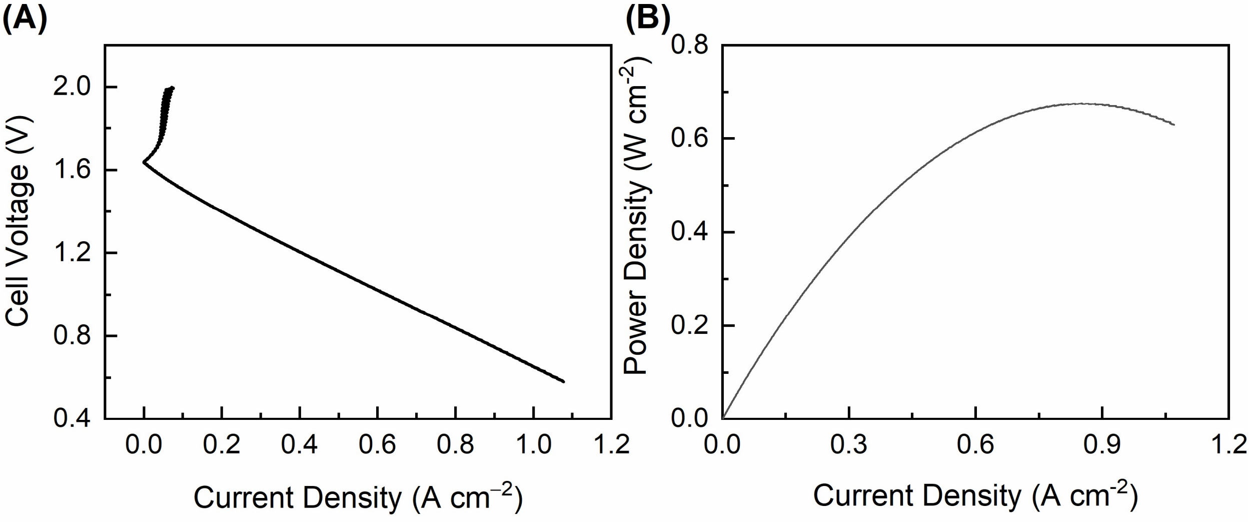

Figure S14: (A) High SOC LSV for a 1.5 M V^{3+} and 1.5 M V^{4+} RFB. (B) Power density curve derived from (A).

5.3 Cell Cycling - Charging and Discharging

Cell cycling is performed utilizing a chronopotentiometry test and involves applying a constant current to charge and discharge the battery while recording the cell voltage as a function of time. Cell cycling can be used to examine coulombic efficiency, voltage efficiency, and energy efficiency as a function of different current densities. There are two test cutoff methods that can be utilized for cell cycling tests, a time cutoff or a voltage cutoff. A time cutoff, which will stop the charge or discharge after a specific amount of time has passed, is useful for galvanostatic charging or discharging the cell to a specific SOC. A voltage cutoff, which will end the chronopotentiometry test after a target voltage is reached, is useful for fully charging or discharging the cell and when trying to avoid a solvent stability window. The charging target cutoff voltages are chosen to correspond to voltage increase spikes that indicate that the cell has fully charged or has begun an unrelated process such as hydrogen production. The discharge voltage cutoff is chosen to correspond to a full discharge of the battery.

An example of a VRFB cycling at various current densities and utilizing voltage cutoffs for both charging and discharging is shown in Figure S15. The curve is dictated by the Sand Equation.[3] The charging cutoff voltage for the described cell was either 2.0 V or 2.1 V depending on current density. The discharge cutoff voltage for the described cell was between 0.3–0.5 V depending on current density. The voltage spikes are demonstrated in the cell cycling figure. As can be seen in the figure, the higher the current density, the larger the overpotentials, requiring higher charging voltages and leading to lower discharge voltages, as well as utilizing less overall capacity of the electrolyte due to the increased difficulty of maintaining the required current. Because current density can impact capacity utilization, it is important that prior to the first cycle at a new current density that a "pre-cycling" cycle is performed at the operating current density in order to set the SOC to the proper operating capacity. For example, if at a specific current density, a cell can only operate between 5–95% SOC, then one would get an artificially low Coulombic efficiency measurement by starting at 0% SOC, charging to 95% SOC, and discharging to only 5% SOC. However, if one runs a pre-cycle to 10% SOC and then back to 5% SOC, the data collection cycle would then start at 5% SOC, and one would get an accurate Coulombic efficiency measurement upon charging to 95% SOC and back to 5% SOC. Cell cycling figures typically show cell voltage as the y-axis and either time or capacity on the x-axis.

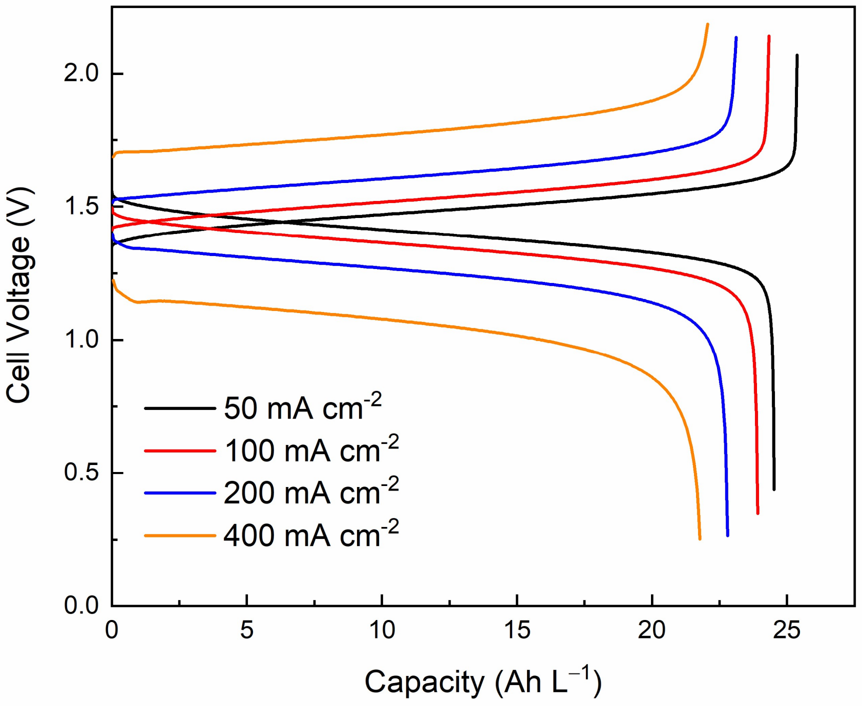

Figure S15: Single charge and discharge curves for a 1.5 M V^{3+} and 1.5 M V^{4+} RFB in 3.5 M H_2SO_4 at various current densities.

It is also possible to charge or discharge an RFB utilizing a constant voltage hold, known as chronocoulometry. This typically is only used to fully charge or discharge the battery after a constant current charge or discharge, because the current will change throughout the voltage hold and does not allow for easy determination of coulombic efficiencies or other performance metrics.

Cell cycling is also often performed for multiple cycles to see if the cycle characteristics (voltage profile or cycle time) change over time or if the electrolyte capacity decreases over time. When running repeated cycling at a specific current density, a decrease in cycle time as the test progresses is an indication of capacity loss and may be indicative of active species instability or active material transport through the membrane. Further testing is required to determine which electrolyte (negolyte or posolyte) is causing the capacity decrease and what is occurring to that electrolyte to cause the decrease. When running repeated cycling tests, plots are typically made showing capacity or an efficiency on the y-axis, and cycle number or time on the x-axis.

5.4 Open Circuit Voltage

An OCV measurement is a standard test that can be performed and will give the voltage difference between the negolyte and posolyte of the assembled RFB when no current is flowing externally through the potentiostat. The OCV value shows the thermodynamic driving force between the negolyte and posolyte.

One typical test that utilizes OCV is an OCV vs. SOC test to plot the voltage of the battery as a function of the SOC of one of the electrolytes. If the volume and concentration of an electrolyte is known, a constant current charge could be performed for a specific amount of time followed by an OCV measurement for 15–30 seconds. This RFB charge for a set time to a specific SOC followed by OCV measurement is repeated until you get data for how the voltage changes for a specific SOC (i.e. 5–95% SOC in 5% intervals). This test would expect to show a Nernstian dependence as the SOC changes (Equation 1). A typical OCV vs SOC plot will have the y-axis as OCV and the x-axis as SOC with data points plotted representing the OCV measured at specific SOC values. An example of this plot generated from the Nernst Equation and the initial starting concentration of vanadium from this guide is shown below in Figure S16. Note that by increasing the H^+ concentration, the OCV of the cell can actually be manipulated higher than the theoretical OCV based on standard reduction potentials.

$$E = E^0 - 0.0592\,V \times \log_{10}\left(\frac{[V^{3+}]\,[VO^{2+}]}{[V^{2+}]\,[VO_2^+]\,[H^+]^2}\right) \tag{1}$$

Another OCV test that can be performed is long-term OCV measurement of charged or discharged electrolytes. Monitoring the OCV over a long period of time (e.g. 1 hour or longer) can show if there is a change in the charge state or composition of the electrolytes. Seeing an increase or decrease in the OCV over time would indicate that somehow the system is changing and could suggest a variety of phenomena occurring such as active-species instability (decomposition, dimer-formation, reactivity with solvent, etc.), active-species membrane crossover and self-discharge, difference in solubility for charged/discharged species, or even system level air leaks for air sensitive species. Further testing to determine the exact source of OCV change is required beyond the scope of this work, but the long term OCV test can be useful as a quick preliminary test for long-term electrolyte stability.

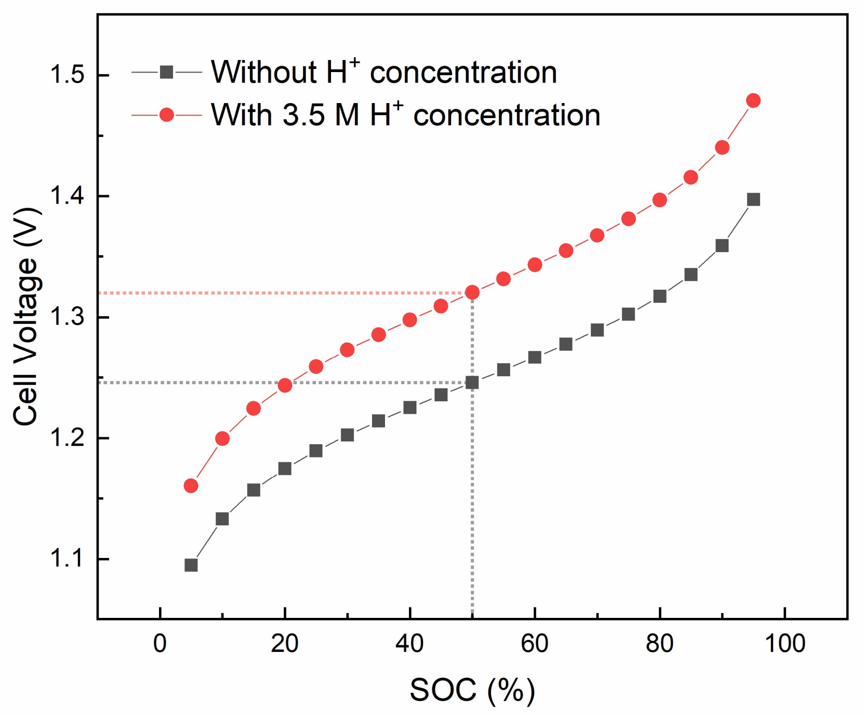

Figure S16: Theoretical cell voltage versus SOC for a 1.5 M V^{3+} and 1.5 M V^{4+} RFB. Black represents the theoretical curve with no H^+ concentration dependence in the Nernst Equation (1 M H^+). Red represents the theoretical curve including both the 3.5 M H^+ concentration and how the H^+ concentration changes during charging (On the catholyte side: 2 H^+ generated and 1 H^+ leaving through the membrane per V^{4+} to V^{5+} charge). The dashed lines show the OCVs at 50% SOC.

5.5 Results

Important results to discuss when reporting RFB data include cell cycling data. Coulombic efficiency investigates, for a single cycle, the coulombs of charge input into the cell compared to the coulombs of charge taken out of the cell. Coulombic efficiency can be calculated by dividing the discharge time of one cycle by the charge time of the same cycle. Coulombic efficiency less than 100% indicates that electrons are being put into the system and not taken out and can be an indication of many possible phenomena occurring, such as electro-active species decomposition, water splitting or hydrogen production, or active species crossover leading to self-discharge.

Voltage efficiency investigates how the charging voltage compares to the discharging voltage. Voltage efficiency for a single cycle can be calculated by dividing the average discharge voltage of the cycle by the average charge voltage of the cycle. This value is can be an indication of overpotentials due to electron transfer kinetics or cell resistance due to factors such as membrane resistance from ion transport.

Energy efficiency compares the total energy put into the battery during charging with the energy retrieved from the battery during discharging. Energy efficiency can be calculated by multiplying the voltage efficiency and the coulombic efficiency. Energy efficiency is a value that can be directly compared to other battery and non-battery forms of energy storage but does not include system level losses for RFBs such as AC/DC conversion losses and pumping losses.

The values of coulombic efficiency, voltage efficiency, and energy efficiency from the VRFB cycling in Figure S15 were calculated and are shown below in Table S1. Note that at high current densities, the cell voltage efficiency drops due to the high overpotentials required. For VRFBs, the high charging overpotential can lead to the cell experiencing voltages up to 2.0 V, which as earlier mentioned with V(V), can lead to carbon oxidation/corrosion and damage the RFB flow plates.

Table S1: RFB cell efficiencies as a function of current density for the 1.5 M VRFB

Current Density (mA cm^{-2})	**400**	**200**	**100**	**50**
Coulombic Efficiency (%)	98.7	98.7	98.3	96.6
Voltage Efficiency (%)	57.6	75.8	86.7	93.0
Energy Efficiency (%)	56.8	74.8	85.2	89.8

Another important result to discuss is the maximum power output of the cell. This allows for the comparison of the maximum power output per unit area for various energy storage methods. For the reported VRFB, the maximum power output, found from the maximum value in Figure S14B, was 675 mW cm^{-2}.

Other forms of data, besides cell cycling and power data, can also be presented in RFB papers depending on the focus of the paper. This is not an exhaustive list of possible tests to run, or data to present, and specific investigations into factors such as active species electrolyte crossover or long term active species stability may require other electrochemical tests that are not detailed here but are demonstrated in the literature.

6. Additional Resources

As previously noted, this guide is meant to demonstrate a basic RFB assembly and electrochemical evaluation using only items that can be purchased directly from suppliers without modification. We have not detailed any sort of cell optimization through membrane or electrodes treatments, nor have we gone into any details about flow field optimization or further electrochemical experiments that can be performed. Here we have provided some additional resources for those interested in further testing and optimizing their RFB chemistry beyond the basics provided in this guide.

Video Tutorials

To further clarify the RFB assembly information provided in this text, additional video instructions for certain aspects of the assembly process can be found at the Marshak Lab YouTube channel:

https://www.colorado.edu/marshakgroup/youtube

Component Optimization (Electrode, Membranes, Temperature):

The type of membranes and electrodes utilized, and the types of pre-treatments performed on those membranes and electrodes, can impact various cell characteristics including electron transfer kinetics, fluid transport properties, overall cell resistance, and active species crossover rate. Therefore, when optimizing the system performance for a particular electrolyte chemistry, it may be important to thoroughly investigate various membranes and electrodes as they can affect properties such as coulombic efficiency, voltage efficiency, energy efficiency, maximum power output, and electrolyte capacity over time. Both electrode and membrane performance can be impacted by temperature. Further reading on prior published literature methods for alternative electrodes and electrode treatments, alternative membranes and membrane treatments, and the impact of temperature can be found in the following sources:

Electrodes

- Carbon Paper Heat Treatments for VRFBs[4,5]
- Overview of Various Types of Carbon Based Electrodes[6]

Membranes

- Membranes to Use for RFBs[7]
- Testing of Nafion 115, 212, 211[8]
- Testing of N112, Fumasep, Aquivion[9]
- Nafion Treatments: Nafion Technical Bulletin No. 93-01

Temperature

- Temperature Effects on Membranes, Efficiency, and Power of FeCr RFBs[10]

Cell Optimization

How the cell itself is assembled and operated can also have impacts on the RFB performance. Various factors of the cell design itself, including the thickness of electrodes utilized, the amount of compression that the cell is under, the flow field design that the graphite flow plate utilizes, and the flow rate of the electrolyte can impact cell efficiencies and maximum power output. For lab scale testing, minimizing pumping cost is often not a priority. Therefore, determining the optimal flow field design and optimal flow rate may not be required, and the fluid is simply flowed at a high enough flow rate to not impact the electrochemical testing. Further reading on prior published literature information for cell design, including electrode thickness, cell compression, and flow field designs can be found in the following sources:

Electrode Thickness and Cell Compression

- Optimized Electrode Configuration – Varying Number of Carbon Paper Layers[11]
- Graphite Felt and Carbon Paper Compression[1]

Flow Field Designs

- Interdigitated Flow Plates[12,13]
- Flow Fields, Stacks, and Design Considerations[14–16]

Additional Electrochemical Testing Procedures

There are other electrochemical testing procedures that can be performed with a RFB setup in order to examine other properties of the electroactive species or of the cell design itself. Further reading on prior published literature information for additional electrochemical testing methods can be found in the following sources:

Additional Electrochemical Methods

- The Cell-in-Series Method: A Technique for Accelerated Electrode Degradation[17]
- Symmetric Cell System Testing for Stability[18]
- Extending Lifetime Through Altered Operating Conditions[19]
- Electrochemical Impedance Spectroscopy (EIS): Investigating RFB Cell Resistances[20,21]
- Use of a Reference Electrode[22]

Other RFB Areas of Consideration

There are other areas of consideration that one may need to investigate when trying to optimize an RFB set up. For instance, some active species may be oxygen sensitive, such as how V^{2+} and V^{3+} will oxidize to V^{4+} when exposed to oxygen. Other species may have long term electrolyte stability issues in specific oxidation states. Below are some additional readings on some other topics that may be important to specific RFB electrolyte chemistries.

Other RFB Areas of Consideration

- Crossover Mitigation Strategies[23]
- Testing for Oxygen Sensitivity of RFB Electrolytes[2,24]
- Utilizing In-Situ UV-Vis Spectrophotometry in an RFB[25]
- Investigating Sources of RFB Capacity Fade[26]
- Transport Property Requirements for RFB Separators[27,28]

7. References

1. Davies, T.J., and Tummino, J.J. (2018). High-Performance Vanadium Redox Flow Batteries with Graphite Felt Electrodes. C *4*, 8.

2. Robb, B.H., Waters, S.E., and Marshak, M.P. (2020). Minimizing Oxygen Permeation in Metal-Chelate Flow Batteries. ECS Trans. *97*, 237–245.

3. Bard, A.J., and Faulkner, L.R. (2000). Electrochemical Methods: Fundamentals and Applications 2nd Ed. (Wiley).

4. Pezeshki, A.M., Clement, J.T., Veith, G.M., Zawodzinski, T.A., and Mench, M.M. (2015). High performance electrodes in vanadium redox flow batteries through oxygen-enriched thermal activation. Journal of Power Sources *294*, 333–338.

5. Greco, K.V., Forner-Cuenca, A., Mularczyk, A., Eller, J., and Brushett, F.R. (2018). Elucidating the Nuanced Effects of Thermal Pretreatment on Carbon Paper Electrodes for Vanadium Redox Flow Batteries. ACS Appl. Mater. Interfaces *10*, 44430–44442.

6. Forner-Cuenca, A., and Brushett, F.R. (2019). Engineering porous electrodes for next-generation redox flow batteries: recent progress and opportunities. Current Opinion in Electrochemistry, S2451910319301668.

7. Prifti, H., Parasuraman, A., Winardi, S., Lim, T.M., and Skyllas-Kazacos, M. (2012). Membranes for Redox Flow Battery Applications. Membranes *2*, 275–306.

8. Reed, D., Thomsen, E., Wang, W., Nie, Z., Li, B., Wei, X., Koeppel, B., and Sprenkle, V. (2015). Performance of Nafion® N115, Nafion® NR-212, and Nafion® NR-211 in a 1 kW class all vanadium mixed acid redox flow battery. Journal of Power Sources *285*, 425–430.

9. Vrána, J., Charvát, J., Mazúr, P., Bělský, P., Dundálek, J., Pocedič, J., and Kosek, J. (2018). Commercial perfluorosulfonic acid membranes for vanadium redox flow battery: Effect of ion-exchange capacity and membrane internal structure. Journal of Membrane Science *552*, 202–212.

10. Lopez-Atalaya, M., Codina, G., Perez, J.R., Vazquez, J.L., and Aldaz, A. (1992). Optimization studies on a Fe/Cr redox flow battery. Journal of Power Sources *39*, 147–154.

11. Liu, Q.H., Grim, G.M., Papandrew, A.B., Turhan, A., Zawodzinski, T.A., and Mench, M.M. (2012). High Performance Vanadium Redox Flow Batteries with Optimized Electrode Configuration and Membrane Selection. J. Electrochem. Soc. *159*, A1246–A1252.

12. Zeng, Y., Li, F., Lu, F., Zhou, X., Yuan, Y., Cao, X., and Xiang, B. (2019). A hierarchical interdigitated flow field design for scale-up of high-performance redox flow batteries. Applied Energy *238*, 435–441.

13. Macdonald, M., and Darling, R.M. (2019). Comparing velocities and pressures in redox flow batteries with interdigitated and serpentine channels. AIChE J *65*, e16553.

14. Ke, X., Prahl, J.M., Alexander, J.I.D., Wainright, J.S., Zawodzinski, T.A., and Savinell, R.F. (2018). Rechargeable redox flow batteries: flow fields, stacks and design considerations. Chemical Society Reviews.

15. Darling, R.M., and Perry, M.L. (2014). The Influence of Electrode and Channel Configurations on Flow Battery Performance. J. Electrochem. Soc. *161*, A1381–A1387.

16. MacDonald, M., and Darling, R.M. (2018). Modeling flow distribution and pressure drop in redox flow batteries. AIChE J *64*, 3746–3755.

17. Pezeshki, A.M., Sacci, R.L., Veith, G.M., Zawodzinski, T.A., and Mench, M.M. (2016). The Cell-in-Series Method: A Technique for Accelerated Electrode Degradation in Redox Flow Batteries. J. Electrochem. Soc. *163*, A5202–A5210.

18. Goulet, M.-A., and Aziz, M.J. (2018). Flow Battery Molecular Reactant Stability Determined by Symmetric Cell Cycling Methods. J. Electrochem. Soc. *165*, A1466–A1477.

19. Goulet, M.-A., Tong, L., Pollack, D.A., Tabor, D.P., Odom, S.A., Aspuru-Guzik, A., Kwan, E.E., Gordon, R.G., and Aziz, M.J. (2019). Extending the Lifetime of Organic Flow Batteries via Redox State Management. J. Am. Chem. Soc. *141*, 8014–8019.

20. Derr, I., Bruns, M., Langner, J., Fetyan, A., Melke, J., and Roth, C. (2016). Degradation of all-vanadium redox flow batteries (VRFB) investigated by electrochemical impedance and X-ray photoelectron spectroscopy: Part 2 electrochemical degradation. Journal of Power Sources *325*, 351–359.

21. Sun, C.-N., Delnick, F.M., Aaron, D.S., Papandrew, A.B., Mench, M.M., and Zawodzinski, T.A. (2013). Probing Electrode Losses in All-Vanadium Redox Flow Batteries with Impedance Spectroscopy. ECS Electrochem. Lett. *2*, A43–A45.

22. Aaron, D.S., Tang, Z., Lawton, J.S., Papandrew, A.P., and Zawodzinski, T.A. (2012). In Situ Single Electrode Studies of an All-Vanadium Redox Flow Battery. ECS Trans. *41*, 43.

23. Perry, M.L., Saraidaridis, J.D., and Darling, R.M. (2020). Crossover Mitigation Strategies for Redox-Flow Batteries. Current Opinion in Electrochemistry.

24. Aziz, M.J., Ji, Y., Goulet, M.-A., Pollack, D.A., Kwabi, D.G., Jin, S., Porcellinis, D.D., Kerr, E.F., and Gordon, R.G. (2019). A Phosphonate-Functionalized Quinone Redox Flow Battery at Near-Neutral pH with Record Capacity Retention Rate. Advanced Energy Materials *9*, 1900039.

25. Tong, L., Chen, Q., Wong, A.A., Gómez-Bombarelli, R., Aspuru-Guzik, A., Gordon, R.G., and Aziz, M.J. (2017). UV-Vis spectrophotometry of quinone flow battery electrolyte for in situ monitoring and improved electrochemical modeling of potential and quinhydrone formation. Phys. Chem. Chem. Phys. *19*, 31684–31691.

26. Kwabi, D.G., Ji, Y., and Aziz, M.J. (2020). Electrolyte Lifetime in Aqueous Organic Redox Flow Batteries: A Critical Review. Chem. Rev.

27. Darling, R., Gallagher, K., Xie, W., Su, L., and Brushett, F. (2016). Transport Property Requirements for Flow Battery Separators. J. Electrochem. Soc. *163*, A5029–A5040.

28. Elgammal, R.A., Tang, Z., Sun, C.-N., Lawton, J., and Zawodzinski, T.A. (2017). Species Uptake and Mass Transport in Membranes for Vanadium Redox Flow Batteries. Electrochimica Acta *237*, 1–11.